Magnetodielectric coupling in frustrated spin systems

Mufti, N.; Nugroho, A. A.; Blake, G. R.; Palstra, T. T. M.

Magnetodielectric coupling in frustrated spin systems: the spinels MCr$_2$O$_4$ (M = Mn, Co and Ni)

N Mufti[1,3], **A A Nugroho**[1,2], **G R Blake**[1] **and T T M Palstra**[1]

[1] Solid State Chemistry Laboratory, Zernike Institute for Advanced Materials,
Rijksuniversiteit Groningen, Nijenborgh 4, 9747AG Groningen, The Netherlands
[2] Faculty of Mathematics and Natural Sciences, Institut Teknologi Bandung, Jl. Ganesha 10,
Bandung 40132, Indonesia

Abstract
We have studied the magnetodieletric coupling of polycrystalline samples of the spinels
MCr$_2$O$_4$ (M = Mn, Co and Ni). Dielectric anomalies are clearly observed at the onset of the
magnetic spiral structure (T_s) and at the 'lock-in' transition (T_f) in MnCr$_2$O$_4$ and CoCr$_2$O$_4$, and
also at the onset of the canted structure (T_s) in NiCr$_2$O$_4$. The strength of the magnetodielectric
coupling in this system can be explained by spin–orbit coupling. Moreover, the dielectric
response in an applied magnetic field scales with the square of the magnetization for all three
samples. Thus, the magnetodielectric coupling in this state appears to originate from the P^2M^2
term in the free energy.

(Some figures in this article are in colour only in the electronic version)

1. Introduction

The materials MCr$_2$O$_4$ (M = Mn, Co and Ni) are ferrimagnetic spinels, in which the M^{2+} cations occupy the tetrahedral (A) sites and the Cr^{3+} cations occupy the octahedral (B) sites. In single-crystal samples, collinear ferrimagnetic ordering occurs at T_c = 51 K, 93 K and 74 K for M = Mn, Co and Ni, respectively. A further magnetic transition occurs at $T_s \sim$ 16 K, 24 K and 31 K, respectively [1, 2]. In CoCr$_2$O$_4$ and MnCr$_2$O$_4$ a short-range-ordered (SRO) spiral component develops, giving a conical magnetic structure below T_s. In NiCr$_2$O$_4$ a collinear antiferromagnetic component appears below T_s. A further 'lock-in' transition occurs at T_f = 13 K for CoCr$_2$O$_4$ and at 14 K for MnCr$_2$O$_4$. The magnetic ground state of spinels with spiral or conical structures can be well described by the parameter u [3]:

$$u = \frac{4\tilde{J}_{BB}S_B}{3\tilde{J}_{AB}S_A}. \qquad (1)$$

Here, $\tilde{J}_{BB}$ and $\tilde{J}_{AB}$ are the nearest-neighbor (NN) interactions involving spins S_A and S_B on the A and B

sites. In this model the AA interaction is assumed to be weak and is neglected. It is important to note that the possible values of u range from 0 to infinity, corresponding to configurations between a Néel ferrimagnetic structure and a state characterized by 'magnetic geometric frustration' (MGF). Below u = 8/9 the magnetic structure is described as a Néel long-range ordered configuration [3]. In the range from u = 8/9 to 1.298 the magnetic ground state is predicted to be a long-range ordered spiral structure and above u = 1.298 this magnetic structure is predicted to become locally unstable, with short-range spiral order realized [1]. For single-crystal samples, the coherence length of the spiral component reaches the order of 10 nm at low temperatures with a propagation vector **q** = (0.59, 0.59, 0) for MnCr$_2$O$_4$ and 3.5 nm with a propagation vector **q** = (0.62, 0.62, 0) for CoCr$_2$O$_4$. The corresponding values of u for MnCr$_2$O$_4$ and CoCr$_2$O$_4$ are 1.5 and 2.0, respectively [1]. In contrast, a collinear antiferromagnetic component appears in NiCr$_2$O$_4$ below T_s, with the propagation vector **q** = (0 0 1) [2]. As discussed later, the value of u for NiCr$_2$O$_4$ is expected to be larger than that of CoCr$_2$O$_4$ due to the smaller A-site magnetic moment. The rather short correlation lengths (less than 10 nm) of these spiral structures are thought to be the result of weak geometrical frustration on the spinel B site;

[3] Permanent address: Department of Physics, Universitas Negeri Malang, Jl. Surabaya 6, Malang 65145, Indonesia.

the magnetic exchange interactions between the A and B sites are weaker than those among the B sites and are insufficient to suppress the MGF that arises naturally from the geometry of the B-site pyrochlore sublattice [1]. Yamasaki *et al* have reported the presence of ferroelectricity in $CoCr_2O_4$ single crystals [4], making it one of the few materials to exhibit the coexistence of ferromagnetic and ferroelectric states. The onset of polarization occurs at T_s along the $[1\bar{1}0]$ direction and the polarization can be reversed by switching the direction of the applied magnetic field. It is to be noted that the polarization in this system is smaller than that of the multiferroic $RMnO_3$ perovskites due to the weak spin–orbit coupling strength of Cr^{3+} ($t_{2g}^3e_g^0$) compared to Mn^{3+} ($t_{2g}^3e_g^1$) [4]. The mechanism of the induced ferroelectricity in $CoCr_2O_4$ can be explained by the spin current model for magnetic ferroelectricity proposed by Katsura *et al* [5]. The relationship between polarization and spin canting for two adjacent spins S_i and S_j can be expressed as $P = ae_{ij} \times (S_i \times S_j)$, where P denotes the induced polarization, e_{ij} is the vector connecting the two spin sites and a is the proportionality constant as determined by the spin–exchange interaction and the spin–orbit interaction [4, 5]. Recently, an unusual relationship between polarization **P**, magnetization **M** and spiral wavevector **q** in this compound has been reported by Choi *et al* [6]. Although switching the sign of a small applied magnetic field reverses the sign of both **P** and **q** (that is, the spiral handedness), on cooling or warming through T_f a polarization reversal is observed with no change in the spiral handedness. These results prompted us to investigate the magnetic and dielectric properties of other members of the series MCr_2O_4. We have already reported a preliminary study of $MnCr_2O_4$ [7]. Here we expand our study to include M = Co and Ni in order to further explore the nature of the magnetodielectric coupling in the spiral (conical) and canted magnetic structures found in this system.

2. Experiment

Polycrystalline samples of MCr_2O_4 (M = Mn, Co and Ni) were prepared by solid state reaction using a stoichiometric mixture of $MnCO_3$, CoO, NiO and Cr_2O_3. The samples were first sintered at 1000 °C for 12 h and then at 1300 °C for 24 h in flowing argon, with intermediate grinding. Magnetization measurements were performed using a Quantum Design MPMS-7 SQUID magnetometer. The capacitance was measured using an Andeen-Hagerling 2500A capacitance bridge at a frequency of 1 kHz and a Quantum Design PPMS. X-ray powder diffraction at room temperature was performed using a Bruker D8 diffractometer operating with Cu Kα radiation.

3. Results

X-ray powder diffraction measurements showed that the MCr_2O_4 (M = Mn, Co and Ni) samples are single phase; $MnCr_2O_4$ and $CoCr_2O_4$ adopt the cubic spinel structure with space group $Fd\bar{3}m$, with lattice parameters of 8.4373(1) Å and 8.3334(1) Å, respectively. In contrast, $NiCr_2O_4$ adopts a tetragonal spinel structure with space group $I4_1/amd$ and

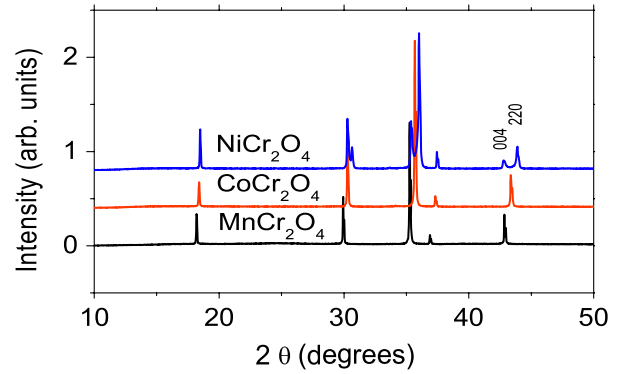**Figure 1.** X-ray powder diffraction patterns of MCr_2O_4 (M = Mn, Co and Ni) at room temperature.

lattice parameters of $a = 5.8351(1)$ Å and $c = 8.4332(1)$ Å. The tetragonal structure is marked by the splitting of Bragg peaks, as shown in figure 1. The lattice parameters of all three samples are in good agreement with those previously reported [8–10]. In spinel MCr_2O_4, M^{2+} occupies the tetrahedral site and Cr^{3+} occupies the octahedral site. In $NiCr_2O_4$ the tetrahedral site containing Ni^{2+} ($e^4t_2^4$) has a Jahn–Teller distortion and is elongated along the c axis, giving rise to the tetragonal structure.

The magnetic susceptibility of MCr_2O_4 (M = Mn, Co and Ni) at different magnetic fields is shown in figure 2. The onset of ferrimagnetic ordering is observed at 43 K for $MnCr_2O_4$, 97 K for $CoCr_2O_4$ and 75 K for $NiCr_2O_4$ in a field of 0.1 T. In all of the samples the value of T_c increases with applied magnetic field and the transition becomes broader. Other anomalies are observed at $T_s \sim 18$ K and $T_f \sim 15$ K for $MnCr_2O_4$ and $T_s \sim 27$ K and $T_f \sim 15$ K for $CoCr_2O_4$, which correspond to the temperatures where the spiral component appears and to the 'lock-in' transition at which the spiral becomes fully developed, as reported by Tomiyasu *et al* [1]. In $MnCr_2O_4$, both anomalies become less well defined when the field is increased, as previously reported [7]. In $CoCr_2O_4$, the anomalies are still visible up to at least 3 T. For $NiCr_2O_4$ only one anomaly is observed at $T_s \sim 31$ K, which corresponds to the onset of the canted antiferromagnetic structure [2]. Similar to $CoCr_2O_4$, this anomaly is not affected by increasing the magnetic field up to 3 T. Figure 3 shows plots of magnetization versus field at various temperatures. The spontaneous magnetizations of $MnCr_2O_4$, $CoCr_2O_4$ and $NiCr_2O_4$ at 5 K are estimated to be approximately 1 μ_B/f.u., 0.15 μ_B/f.u. and 0.2 μ_B/f.u., respectively, by linearly extrapolating the high-field magnetization to zero field. All of these values are in good agreement with those previously reported [1, 2, 8, 11]. These results indicate that, as the magnetic moment on the A sites decreases, the exchange interaction between the A and B sites leads to an increase of the cone angle associated with the A, B1 and B2 sites. According to the theory of Lyons *et al* [3], this is also associated with an increase in the value of u. Larger values of u will result in a greater degree of hysteresis in the magnetization versus field loops.

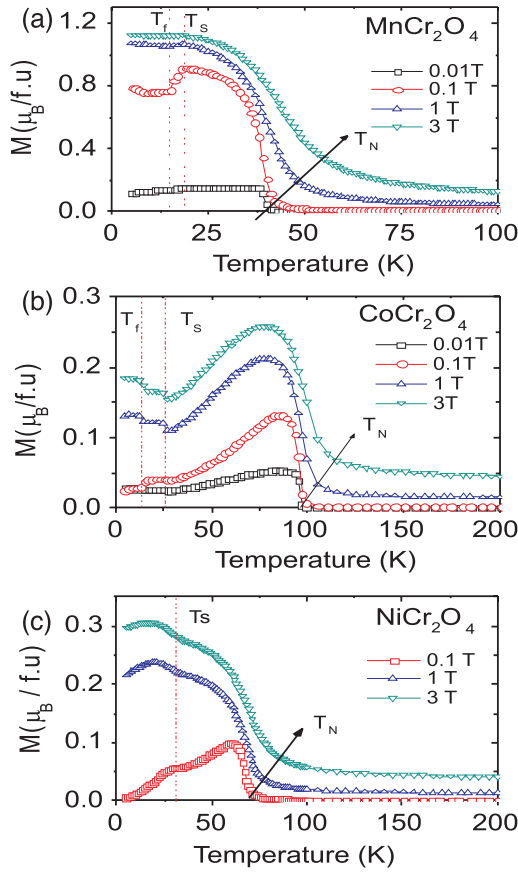The temperature dependence of the dielectric constant of MCr_2O_4 (M = Mn, Co and Ni) is shown in figure 4.

Figure 2. Temperature dependence of magnetization of (a) MnCr$_2$O$_4$ (taken from [7]), (b) CoCr$_2$O$_4$ and (c) NiCr$_2$O$_4$ under different applied magnetic fields. The samples were cooled in zero field (ZFC).

Figure 3. Field dependence of magnetization at various temperatures for (a) MnCr$_2$O$_4$ (taken from [7]), (b) CoCr$_2$O$_4$ and (c) NiCr$_2$O$_4$.

Three anomalies are apparent for MnCr$_2$O$_4$ and CoCr$_2$O$_4$, at approximately the same temperatures as the magnetic transitions. The small differences in transition temperatures are probably due to differences in temperature between the sensor and sample during heating. For MnCr$_2$O$_4$ the temperature dependence of the dielectric constant was reported previously for a high density sample which was pelletized at 600 bar; the dielectric constant increased with decreasing temperature and reached a plateau at 43 K, corresponding to the ferromagnetic transition. The dielectric constant then fell more rapidly at T_f and showed a further anomaly at T_f [7]. In this report we pelletized all three samples at ∼150 bar. The dielectric behavior of MnCr$_2$O$_4$ at T_s and T_f is similar to that previously observed. However, no clear anomaly is seen at the magnetic ordering temperature T_c. The reason for the difference in slope above T_c for the two samples is unclear, but may be due to the difference in density. In this case, extrinsic effects (such as Maxwell–Wagner or polaron relaxation) due to factors such as the electrodes and contacts, grain boundaries and porosity would play a significant role.

The dielectric constant of CoCr$_2$O$_4$ has previously been measured by Lawes *et al* [9]; anomalies were observed at $T \sim 50$ K and $T_s \sim 27$ K and were assigned to the onset of short-range magnetic order and long-range magnetic order, respectively. It was argued using specific heat data that the
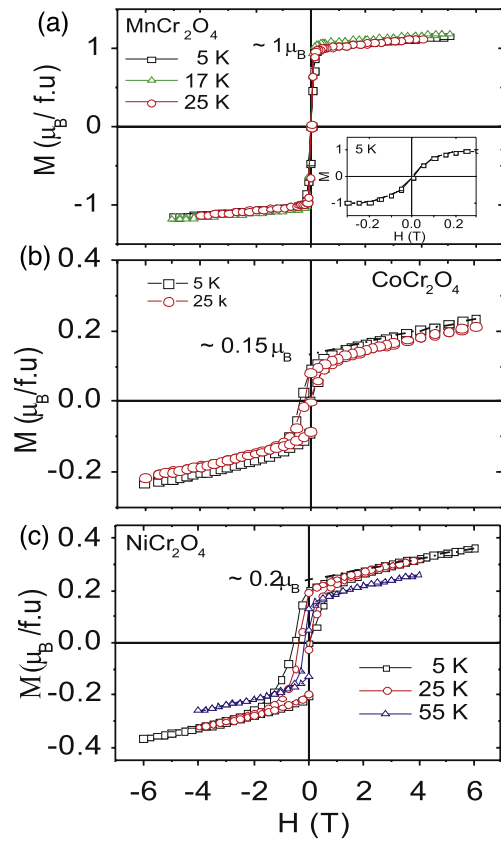
correlation length of the spiral state is different in single-crystal and polycrystalline samples; in the latter a long-range-ordered (LRO) spiral develops below T_s. In contrast, we only observe anomalies at 27 and 15 K (see figure 4(b)); these agree with the onset temperature of the SRO conical structure and the 'lock-in' transition reported by Tomiyasu *et al*, who carried out magnetic measurements and neutron diffraction measurements on single-crystal samples [1]. In NiCr$_2$O$_4$, the temperature dependence of the dielectric constant shows changes in slope at T_c and T_s. The profile remains unchanged on applying magnetic fields of up to 8 T, except for MnCr$_2$O$_4$ at T_f, which is suppressed with increasing magnetic field [7].

Figure 5 shows the magnetocapacitance of the three compounds, that is, the dielectric constant as a function of magnetic field. We define the magnetodielectric response (MD) as MD = $(\varepsilon(H) - \varepsilon(0))/\varepsilon(0)$, where $\varepsilon(H)$ is the dielectric constant under field and $\varepsilon(0)$ is the dielectric constant in the absence of any magnetic field. For MnCr$_2$O$_4$, the dielectric constant suddenly drops (negative magnetocapacitance) in very low magnetic fields. Moreover, the unusual magnetocapacitance profile develops an asymmetric shape below T_f; it is symmetric at temperatures above T_s. In contrast, the magnetodielectric profiles of CoCr$_2$O$_4$ and NiCr$_2$O$_4$ indicate a sharp increase in the dielectric constant in low magnetic fields, and are symmetric at all temperatures. The magnitude of the magnetodielectric response increases in the order MnCr$_2$O$_4$, CoCr$_2$O$_4$ and NiCr$_2$O$_4$.
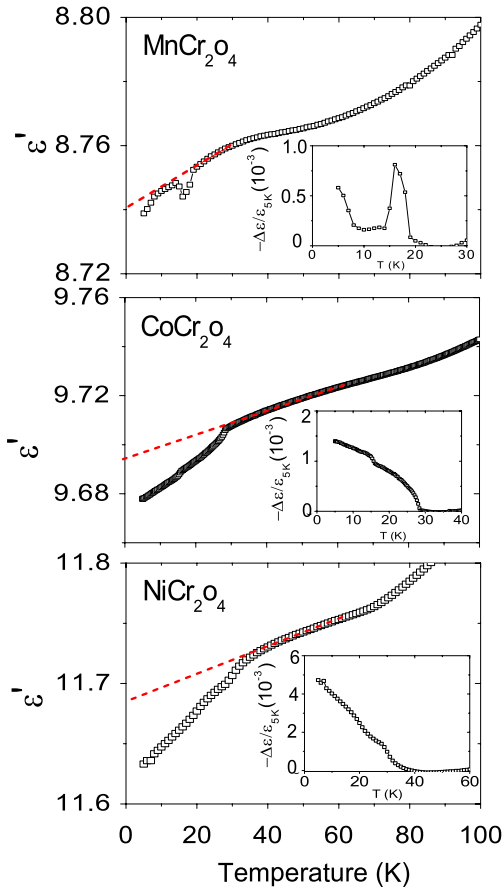
Figure 4. Temperature dependence of the dielectric constant of MCr_2O_4 (M = Mn, Co and Ni). The insets show the negative of the residual dielectric constant after subtraction of the linearly extrapolated value and division by the dielectric constant at 5 K ($-\triangle\varepsilon/\varepsilon_{5\,K}$).
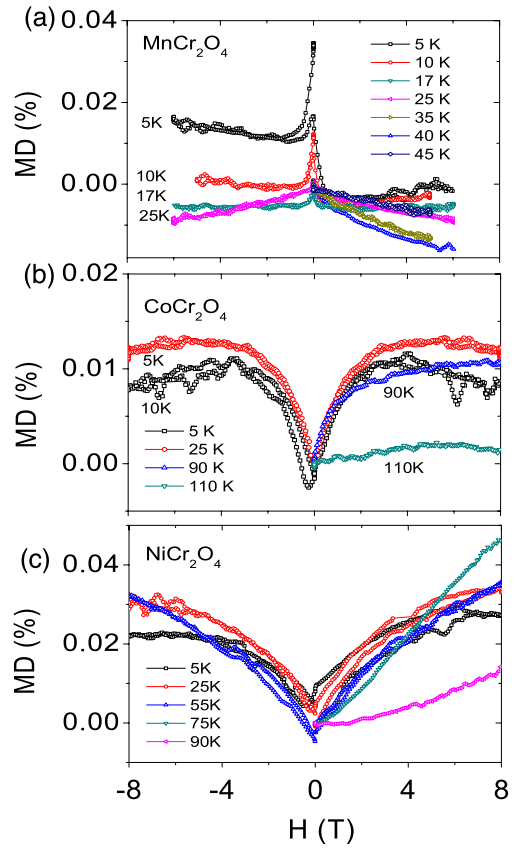

Figure 5. Dielectric constant as a function of magnetic field (in the form of magnetodielectric response—see the text for a definition) for (a) $MnCr_2O_4$, (b) $CoCr_2O_4$ and (c) $NiCr_2O_4$.

4. Discussion

In order to investigate the magnetodielectric coupling in spinel MCr_2O_4 (M = Mn, Co and Ni), we consider the trend of the dielectric constant below T_s. Because MCr_2O_4 is non-polar between T_c and T_s [4], we have taken a linear extrapolation of the dielectric constant from this region down to low temperature. The insets in figure 4 show the residual dielectric constant after subtraction of the linearly extrapolated values and division by the dielectric constant at 5 K ($-\triangle\varepsilon/\varepsilon_{5\,K}$). The residual dielectric constant, that is, the deviation from the extrapolated value, increases in the order $MnCr_2O_4$, $CoCr_2O_4$ and $NiCr_2O_4$. The magnitude of the residual dielectric constant corresponds to the magnetodielectric coupling strength; thus large deviation from the linearly extrapolated values indicates large magnetodielectric coupling. In order to explain this phenomenon, we consider the spin–orbit coupling of M^{2+}. The spin–orbit coupling is defined as $\lambda L \cdot S$, where L is the orbital angular momentum and S is the total spin. In $MnCr_2O_4$, Mn^{2+} (d^5) has $L = 0$, hence no spin–orbit coupling. For $CoCr_2O_4$, Co^{2+} (d^7) has $\lambda = -177$ cm^{-1} [12] in tetrahedral crystal fields; the orbital moment is not fully quenched as recently observed for $Zn_{1-x}Co_xCr_2O_4$ [15] and spin–orbit coupling can affect the

magnetodielectric coupling. For $NiCr_2O_4$, the Ni^{2+} cation (d^8) has a larger spin–orbit coupling constant $\lambda = -315$ cm^{-1} [12] in tetrahedral coordination. For this system we observe the largest magnetodielectric coupling.

The LRO ferrimagnetic structure and the SRO spiral structure are known to coexist below T_f in $MnCr_2O_4$ and $CoCr_2O_4$. In $MnCr_2O_4$, there are two sets of spiral domains with propagation vectors parallel to the [110] and [$\bar{1}$10] directions for an easy axis parallel to [1$\bar{1}$0]. In contrast, $CoCr_2O_4$ has four spiral domains with propagation vectors $\pm$[110] and $\pm$[1$\bar{1}$0] for an easy axis along the [001] direction [1]. Moreover, the correlation length of the spiral in single-crystal $MnCr_2O_4$ (9.9 nm) is larger than that in $CoCr_2O_4$ (3.1 nm). This difference might cause the dielectric anomaly at T_f to be more pronounced in $MnCr_2O_4$ than in $CoCr_2O_4$. However, we note that the origin of the dielectric anomaly at T_f is somewhat unclear; although different studies agree that a 'lock-in' of the **q** vector takes place here, in addition Choi *et al* recently observed a reversal of the polarization at T_f for $CoCr_2O_4$ single crystals, where the handedness of the spiral did not change [6]. In contrast, an earlier study by Yamasaki *et al* on single-crystal $CoCr_2O_4$ revealed only a small anomaly in **P** at T_f [4], pointing at a probable sample dependence. These reports, combined with the difference in magnetic domain structures between $MnCr_2O_4$ and $CoCr_2O_4$ and the possibility that the spiral phase in polycrystalline

samples of MCr_2O_4 is coherent over a longer range than that in single crystals [7, 9], makes it difficult to compare the dielectric anomalies of our samples at T_f in a meaningful manner. This also applies to our observation that the T_f anomaly in $MnCr_2O_4$ is suppressed with applied field [7]; one would expect the correlation length of the spiral structure to increase with field as the sample becomes more single domain in nature, perhaps making the dielectric anomaly more pronounced. For $CoCr_2O_4$ the anomaly at T_f is much smaller, hence it is difficult to observe any change on the application of a magnetic field. The asymmetric magnetodielectric behavior in $MnCr_2O_4$ is also difficult to explain. One possibility is due to a strong coupling of the Mn^{3+} spins to the lattice, which makes the spin system relatively rigid during rotation of the magnetization. The spins deviate by the smallest possible angle from their local easy axes, which determines the most favorable spin configuration. Therefore, the energy of the spin configuration will change when the sign of the magnetization changes and thus dielectric asymmetry is observed [16]. A similar phenomenon has previously been observed in Mn_3O_4, for which it was argued that the asymmetry is due to the magnetic hysteresis present at low temperatures [13]. However, we believe that this argument is not relevant in the case of $MnCr_2O_4$ because we do not observe magnetic hysteresis in our magnetization measurements. Moreover, in $CoCr_2O_4$ and $NiCr_2O_4$ where magnetic hysteresis is observed, the magnetodielectric behavior is symmetric. Further investigation of the magnetodielectric response on single crystals might give a better understanding of these phenomena.

In figure 6 we superimpose plots of the magnetodielectric response and the square of the magnetization for all three samples. The two types of plot overlie each other more closely for $MnCr_2O_4$ than for $CoCr_2O_4$ and $NiCr_2O_4$. Nevertheless, the magnetodielectric $(-\triangle\varepsilon/\varepsilon_{H=0})$ response scales approximately with the square of the magnetization (M^2) for all three samples. This suggests that the magnetodielectric coupling originates from the P^2M^2 term in the free energy expansion, which is always allowed by symmetry in ferroelectromagnetic materials [14]. The magnitude of the magnetodielectric response $(-\triangle\varepsilon/\varepsilon_{H=0})$ increases in the order $MnCr_2O_4$, $CoCr_2O_4$ and $NiCr_2O_4$. This result is consistent with the residual dielectric constant $(-\triangle\varepsilon/\varepsilon_{5\,K})$ at low temperatures in figure 4. Nevertheless, the magnetodielectric effect in these spinel materials is small compared to other multiferroics such as $TbMnO_3$, which has a magnetocapacitance of 10%, even though the ferroelectricity in $MnCr_2O_4$ and $CoCr_2O_4$ is also induced by the magnetic structure. This result indicates that improper ferroelectricity, such as ferroelectricity induced by the magnetic structure, is no guarantee of obtaining a large magnetodielectric effect.

5. Conclusion

We have investigated the magnetic and dielectric properties of polycrystalline samples of the spinels MCr_2O_4 (M = Mn, Co and Ni). Coupling between the dielectric and magnetic properties is observed at the onset of the magnetic spiral structure (T_s) and at the 'lock-in' transition (T_f) in $MnCr_2O_4$ and $CoCr_2O_4$, and also at the onset of the canted structure
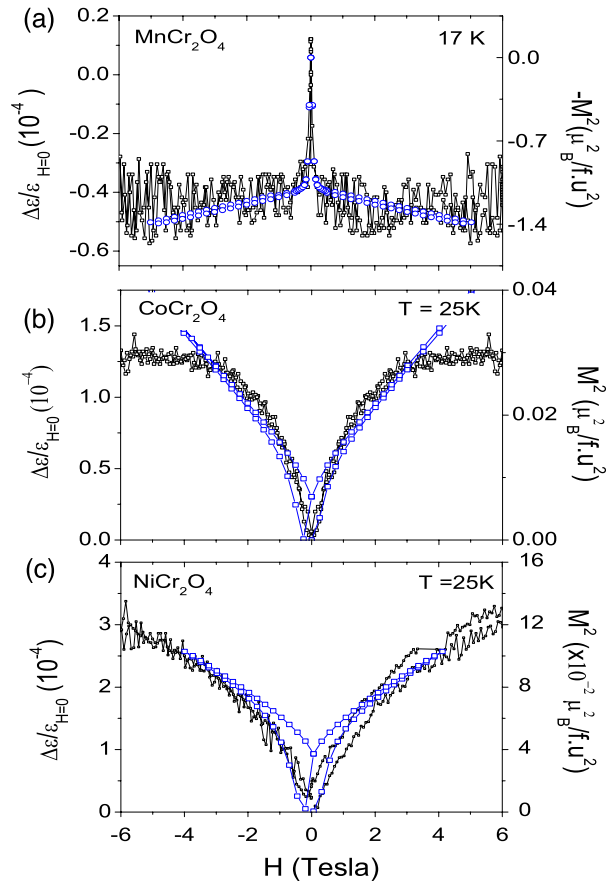

Figure 6. Magnetodielectric response (black data points) and the square of the magnetization (colored data points) as a function of magnetic field for (a) $MnCr_2O_4$, (b) $CoCr_2O_4$ and (c) $NiCr_2O_4$.

(T_s) in $NiCr_2O_4$. The strength of the magnetodielectric coupling in this system can be explained by taking into account the relative strengths of the spin–orbit coupling in the three materials. The magnetodielectric response in applied magnetic fields scales with the square of the magnetization for all three samples. Although the ferroelectricity in this system is related to the linear term $(PM\partial M)$, the magnetodielectric coupling in this state appears to originate from the P^2M^2 term in the free energy. The magnetodielectric effect in all three MCr_2O_4 materials is very small, which implies that frustrated materials showing magnetically induced ferroelectricity do not necessarily exhibit large magnetodielectric effects.

References

[1] Tomiyasu K, Fukunaga J and Suzuki H 2004 *Phys. Rev.* B **70** 214434
[2] Tomiyasu K and Kagomiya I 2004 *J. Phys. Soc. Japan* **73** 2539
[3] Lyons D H, Dwight K, Kaplan T A and Menyuk N 1962 *Phys. Rev.* **126** 540
[4] Yamasaki Y, Miyasaka S, Kaneko Y, He J-P, Arima T and Tokura Y 2006 *Phys. Rev. Lett.* **96** 207204
[5] Katsura H, Nagaosa N and Balatsky A V 2005 *Phys. Rev. Lett.* **95** 057205
[6] Choi Y J, Okamoto J, Huang D J, Chao K S, Lin H J, Chen C T, van Veenendaal M, Kaplan T A and Cheong S-W 2009 *Phys. Rev. Lett.* **102** 067601
[7] Mufti N, Blake G R and Palstra T T M 2008 *J. Magn. Magn. Mater.* **321** 1767

[8] Hastings J M and Corliss L M 1962 *Phys. Rev.* **126** 556
[9] Lawes G, Melot B, Page K, Ederer C, Hayward M A,
      Proffen Th and Seshadri R 2006 *Phys. Rev.* B **74** 024413
[10] Prince E 1961 *J. Appl. Phys.* **32** 68S
[11] Bhowmik R N, Ranganathan R and Nagarajan R 2006 *Phys. Rev.* B **73** 144413
[12] Housecroft C E and Sharpe A G 2008 *Inorganic Chemistry* 3rd edn (Harlow: Prentice-Hall)
[13] Tackett R, Lawes G, Melot B C, Grossman M, Toberer E S and Seshadri R 2007 *Phys. Rev.* B **76** 024409
[14] Kimura T, Kawamoto S, Yamada I, Azuma M, Takano M and Tokura Y 2003 *Phys. Rev.* B **67** 180401
[15] Melot B C, Drewes J E, Seshadri R, Stoudenmire E M and Ramirez A P 2009 *J. Phys.: Condens. Matter* **21** 216007
[16] Krupička S, Jirăk Z, Novăk P, Roskovec V and Zounovă F 1977 *Physica* B **86–88** 1459